velocity to the inviscid flow. In fact, according to the inviscid solution developed herein, the profile is linear, $ru = r(1-z)$, the inviscid flow being rotational.

EXPERIMENTAL COMPARISONS

Velocity profiles have been measured in two experiments cited previously [6, 7]. Each design had attributes not completely in accord with the systems analyzed herein; the experiment with the internal viscous layer [6] had injection Reynolds numbers in the vicinity of 20, which is sufficiently small for effects of heat conduction on velocities to be measurable, and that with the boundary layer on the burning carbon surface [7] employed an open tube instead of a porous wall, giving a nonzero axial pressure gradient near the injection plane. Approximate corrections for these differences resulted in good agreement between theoretical calculation and measurement [14].

Acknowledgement—This work was supported by the National Science Foundation through its program on Research Applied to National Needs, Grant No. AEN-75-20997.

REFERENCES

1. I. Proudman, An example of steady laminar flow at large Reynolds number, *J. Fluid Mech.* **9**, 593–602 (1960).
2. R. M. Terrill, Heat transfer in laminar flow between parallel porous plates, *Int. J. Heat Mass Transfer* **8**, 1491–1497 (1965).
3. J. H. Kent and F. A. Williams, Extinction of laminar diffusion flames for liquid fuels, in *Fifteenth Symposium (International) on Combustion*, pp. 315–325. The Combustion Institute, Pittsburgh (1975).
4. K. Seshadri and F. A. Williams, Effect of CF_3Br on counterflow combustion of liquid fuel with diluted oxygen, *ACS Symposium Series* No. 16, *Halogenated Fire Suppressants*, pp. 149–182. American Chemical Society, Washington, D.C. (1975).
5. K. Seshadri and F. A. Williams, Structure and extinction of counterflow diffusion-flames above condensed fuels: Comparison between polymethylmethacrylate and its liquid monomer, both burning in nitrogen–air mixtures, submitted for publication.
6. T. P. Pandya and N. K. Srivastava, Structure of counterflow diffusion flame of ethanol, *Combust. Sci. Technol.* **11**, 165–180 (1975).
7. K. Matsui, A. Kôyama and K. Uehara, Fluid-mechanical effects on the combustion rate of solid carbon, *Combust. Flame* **25**, 57–66 (1975).
8. R. B. Bird, W. E. Stewart and E. N. Lightfoot, *Transport Phenomena*. Wiley, New York (1960).
9. A. Liñán, The asymptotic structure of counterflow diffusion flames for large activation energies, *Acta Astronautica* **1**, 1007–1039 (1974).
10. L. Krishnamurthy, F. A. Williams and K. Seshadri, Asymptotic theory of diffusion-flame extinction in the stagnation-point boundary layer, *Combust. Flame* **26**, 363–377 (1976).
11. D. R. Kassoy, On laminar boundary layer blowoff, *J. Soc. Ind. Appl. Math.* **18**, 29–40 (1970).
12. P. A. Libby, Numerical analysis of stagnation point flows with massive blowing, *AIAA Jl* **8**, 2095–2096 (1970).
13. L. Krishnamurthy and F. A. Williams, A flame sheet in the stagnation-point boundary layer of a condensed fuel, *Acta Astronautica* **1**, 711–736 (1974).
14. K. Seshadri, Studies of flame extinction, Ph.D. Thesis, University of California, San Diego, La Jolla, CA (1977).

Int. J. Heat Mass Transfer. Vol. 21, pp. 253–256. Pergamon Press 1978. Printed in Great Britain

THE DEVELOPMENT OF A MODEL FOR THREE-DIMENSIONAL FLOW IN TUBE BUNDLES

D. Butterworth
Heat Transfer and Fluid Flow Service, AERE Harwell, Oxon OX11 0RA, U.K.

(*Received* 18 *February* 1977 *and in revised form* 23 *May* 1977)

NOMENCLATURE

- D, tube outside diameter [m];
- g_i, component of gravitational acceleration in direction x_i [m/s²];
- k, isotropic flow conductivity [m²];
- K_{ij}, flow conductivity tensor [m²];
- K_i', flow conductivity in principal direction [m²];
- L, length of bundle measured in flow direction [m];
- p, pressure [Pa];
- R_{ij}, flow resistance tensor [m⁻²];
- Re, Reynolds number defined by $\rho|\mathbf{u}|D/\mu$;
- t, time [s];
- u_i, component of superficial velocity in direction x_i [m/s];
- U, bundle approach velocity [m/s];
- x_i, rectangular coordinate [m];
- X, transverse pitch [m];
- Y, longitudinal pitch [m].

Greek symbols

- α, angle of rotation of axes;
- Δp, pressure drop [Pa];
- ε, porosity or bundle void fraction;
- μ, fluid viscosity [Ns/m²];
- ρ, fluid density [kg/m³].

1. INTRODUCTION

The prediction of the velocity and pressure fields for flow outside tubes (or rods) arranged in regular arrays is of considerable practical importance in the design of certain types of heat-transfer equipment. The purpose of this note is to show how pressure drop data for one-dimensional flow in tube bundles may be generalized in order to provide a framework for analyzing the real flow problems which are often multidimensional in nature. The proposed equations are extensions to those previously used for analyzing flow in anisotropic porous media. This approach does not give very fine detail of the flow field, such as the local velocity profile between a pair of tubes, but instead gives the general trends in pressure and superficial velocity across the bundle. This is all that is necessary in many applications and is perhaps all that can be realistically calculated given the current understanding of multidimensional flow in tube bundles.

2. GENERAL ANALYSIS

Flow in anisotropic porous media is generally [1] represented by equations of the following form:

$$u_i = -\frac{1}{\mu}\sum_j K_{ij}\frac{\partial p}{\partial x_j} \tag{1}$$

where u_i is the superficial velocity in direction x_i and K_{ij} is the permeability tensor. An inverse form of equation (1) may be written as

$$\frac{\partial p}{\partial x_i} = -\mu\sum_j R_{ij}u_j \tag{2}$$

where R_{ij} is a flow-resistance tensor which is related to K_{ij} by

$$\sum_k K_{ik}R_{kj} = \delta_{ij} \tag{3}$$

where δ_{ij} is the Kronecker delta.

For the low Reynolds numbers encountered in porous media calculations, the tensor components K_{ij} and R_{ij} are constants. However, the turbulence encountered in most tube-bundles means that the components depend on the magnitude and direction of the superficial velocity vector $\mathbf{u}$. A convenient simplifying assumption is made here that K_{ij} (and R_{ij}) depend only on the magnitude of the velocity and not the direction. This assumption is shown below to be in reasonable agreement with experimental data. To avoid confusion between the variable K_{ij} and the constant permeability tensor, the former will be referred to as the flow conductivity in the remainder of this note.

The above equations neglect gravitational and inertial forces which have been included [2] for isotropic porous media as follows:

$$\frac{\rho}{\varepsilon}\left(\frac{\partial u_i}{\partial t}+\sum_j u_j\frac{\partial u_i}{\partial x_j}\right)+\frac{\partial p}{\partial x_i} = -\mu\sum_j R_{ij}u_j+\rho g_i. \tag{4}$$

The same form of these terms is assumed valid here.

The above equation is the general momentum equation for flow in rod bundles which should be solved in conjunction with the mass continuity equation which for incompressible flow is

$$\sum_j\frac{\partial u_j}{\partial x_j} = S. \tag{5}$$

The source term S is included for generality but would be zero in many applications. An important potential application [3] of this type of modelling is the analysis of steam flow in power-station condensers. In this case S would be negative.

With the above assumption that the K_{ij} are independent of the flow direction, it can be shown [1] that there are three mutually orthogonal directions which, when the coordinate directions are in line with these directions, have the property that

$$K_{ij} = 0 \quad \text{for} \quad i \neq j.$$

These directions are known as principal directions and the corresponding flow conductivities, K_{ii}, known as principal conductivities. The principal conductivities K_{ii} are denoted by K'_i in the remainder of this note. By symmetry, it is clear that one of the principal directions is parallel to the tubes. For regular arrays, the other two principal directions are along lines of symmetry. For example, in inline arrays, the principal axes are parallel to the rows of tubes.

The transformation rules for rotation about one of the principal directions (x'_3 say) are [1]

$$K_{11} = K'_1\cos^2\alpha + K'_2\sin^2\alpha \tag{6}$$

$$K_{22} = K'_1\sin^2\alpha + K'_2\cos^2\alpha \tag{7}$$

$$K_{21} = K_{12} = (K'_2 - K'_1)\sin\alpha\cos\alpha \tag{8}$$

where α is the angle between the new axes and the principal axes. These same rules apply if K_{ij} are replaced by R_{ij}.

For a wide range of tube arrangements, existing correlations and design charts for pressure drop in tube bundles may be easily transformed to give the principal conductivities as a function of $|\mathbf{u}|$. An excellent compilation of design curves for crossflow is that of ESDU [4]. For axial flow, the hydraulic mean diameter concept may be used, at least to a first approximation, to give the relationship between the axial conductivity and the superficial velocity.

3. CONFIRMATION OF THE MODEL

3.1. *Flow perpendicular to tubes arranged in square and equilateral triangular layouts*

Clearly, in a square array of tubes

$$K'_1 = K'_2 \; (= k \text{ say}) \tag{9}$$

It follows from equations (6)–(8) that

$$K_{11} = K_{22} = k \tag{10}$$

and

$$K_{21} = K_{12} = 0 \tag{11}$$

for all α. Hence, the flow properties in the plane perpendicular to the tubes are isotropic. For tubes arranged in an equilateral-triangle layout, the equations must remain the same after rotation of the axes through 60°. Equations (6)–(8) only admit this possibility if the flow properties are again isotropic. There are data on flow in different directions through square and equilateral triangle arrays which may be

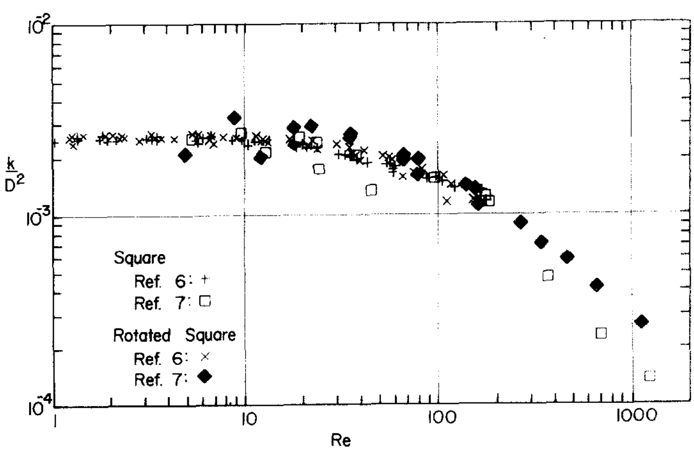

FIG. 1. Flow-conductivity results obtained for flow in two directions in a square array with pitch-to-diameter ratio of 1.25.

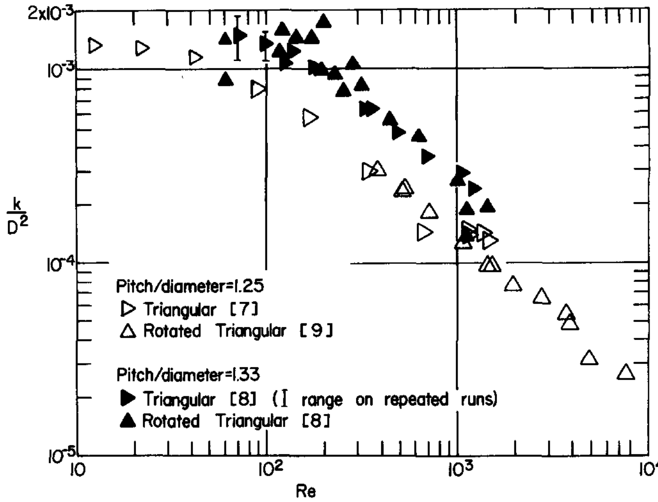

FIG. 2. Flow-conductivity results obtained for flow in two directions in equilateral-triangle arrays with pitch-to-diameter ratios of 1.25 and 1.33.

used to confirm these results. In the following discussion of these data, the definitions proposed by TEMA will be used to denote the tube layout and flow direction.

Figure 1 shows values of k determined from flow in two directions in a square array of pitch-to-diameter ratio 1.25. Similar data are shown in Fig. 2 for equilateral triangular arrays with pitch-to-diameter of 1.25 to 1.33. In these figures, the Reynolds number, Re, is a scalar defined by

$$Re = \rho|\mathbf{u}|D/\mu. \tag{12}$$

It can be seen that, for the most part, the differences in k for the two flow directions are within the scatter in the data. The exception is the square array over the Reynolds number range 300–2000 where there is some indication of a systematic difference between flow directions. However, this difference is small compared with the scatter in the data and hence we are justified in ignoring it until further information is obtained. The general conclusion is therefore that square and equilateral triangle arrays exhibit isotropy in the plane perpendicular to the tube axes which is in agreement with the proposed model.

3.2. *Flow in the plane parallel to the tubes*

Data are available on pressure drop over inclined bundles and this may be compared with predictions from the current model. In the following analysis of this problem, direction 1 is taken as parallel to the tubes and 2 as a principal direction perpendicular to the tubes.

For one-dimensional flow perpendicular to the tubes (case A) the pressure drop is given from equation (1) as

$$\Delta p_A = \mu U L_A / K_2' \tag{13}$$

where U is the approach velocity and L_A the depth of the bundle in the flow direction. The pressure drop for the same bundle when inclined to the flow (case B) is given from equation (2) as

$$\Delta p_B = \mu U L_B R_{22}. \tag{14}$$

The length L_B is related to L_A by

$$L_A = L_B \cos\alpha \tag{15}$$

where α is the angle which the bundle is rotated from the normal flow direction. A pressure drop is also set up normal to the flow direction but this is ignored here since it has not been measured. Combining equations (13)–(15), and using the tensor transformation rules from equations (6)–(8), gives,

$$\frac{\Delta p_B}{\Delta p_A} = \cos\alpha + \frac{K_2'}{K_1'}\sin\alpha\tan\alpha. \tag{16}$$

For values of Re greater than about 10^3 and for the tube layouts usually found in heat exchangers, K_2'/K_1' is very small which means that equation (16) is well approximated by

$$\Delta p_B/\Delta p_A = \cos\alpha \tag{17}$$

for $\alpha \leqslant 60°$.

Kazakevich [10] has obtained pressure drop data for high-Reynolds-number flow over inclined bundles which may be compared with equation (17). These data are unfortunately for only 5 and 6 rows crossed which means that flow-development effects are most likely present in the experiments.

Figure 3 shows the pressure drop ratio, $\Delta p_B/\Delta p_A$, obtained by Kazakevich for each row and the development effect can be seen in these data. The predictions from equation (17) are also shown in this figure and there is some tendency for the measured values to approach the prediction as the number of rows is increased. Hence, those results give further partial support for the model.

4. CONCLUSIONS

General equations are proposed for predicting multidimensional flow in tube bundles. The equations use a flow conductivity (or flow resistance) tensor which may be

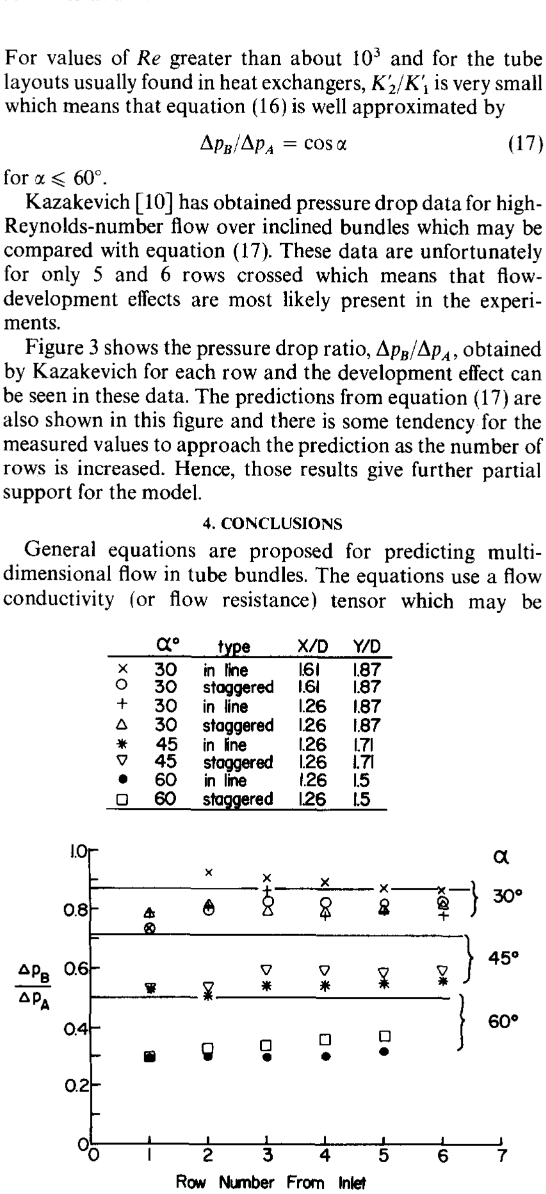

FIG. 3. Comparison of the predicted pressure-drop ratio with the data of Kazakevich [10] for flow over inclined bundles.

obtained from existing correlations for one-dimensional flow through tube bundles. A simple assumption is used that the flow conductivity tensor depends only on the magnitude of the superficial velocity vector and *not* on its direction. This leads to some useful and interesting results, one of which is that the flow properties are isotropic for the plane perpendicular to tubes which are arranged in square and equilateral-triangle arrays. This means that the pressure drop for flow in one direction through such arrays may be predicted from data on the flow in another direction. The assumption that the flow conductivity is independent of flow direction is shown to be in reasonable agreement with existing experimental data.

REFERENCES

1. J. Bear and D. Zaslavsky, *Physical Principals of Water Percolation and Seepage*, edited by S. Irmay. UNESCO, New York (1968).
2. C. S. Yih, *Dynamics of Nonhomogeneous Fluids*, McMillan, New York (1965).
3. Steam turbine condensers, NEL Report No. 619, National Engineering Laboratory, East Kilbride, Glasgow (1976).
4. Pressure loss during crossflow of fluids with heat transfer over plain tube banks without baffles, ESDU Item No. 74040, Engineering Sciences Data Unit, Regent St, London (1974).
5. *Standards of the Tubular Exchanger Manufacturers Association*, 5th edn. TEMA, New York (1968).
6. O. P. Bergelin, A. P. Colburn and H. L. Hull, Heat transfer and pressure drop during viscous flow across unbaffled tube banks, University of Delaware Engineering Experimental Station, Bulletin 2 (1950).
7. O. P. Bergelin, M. D. Leighton, W. L. Lafferty and R. L. Pigford, Heat transfer and pressure drop during viscous and turbulent flow across unbaffled tube banks, University of Delaware Engineering Experimental Station, Bulletin 4 (1958).
8. *Distillation Digest*, Vol. 1 and 2, pp. 279–286, OSW R and D Progress Report, No. 538 (1970).
9. J. E. Deihl and C. H. Unruh, Two phase pressure drop for horizontal crossflow through tube banks, ASME paper 58-HT-20 (1958).
10. F. P. Kazakevich, Influence of the angle of approach of a gas stream on the aerodynamic resistance of a tube bundle, *Izv. Vses. Teplotekh. Inst. Imoni. F.E. Dzerzhinkogo*, No. 8, 7–12 (1952).

Int. J. Heat Mass Transfer. Vol. 21, pp. 256–258. Pergamon Press 1978. Printed in Great Britain

NATURAL CONVECTION FILM BOILING FROM SPHERES TO SATURATED LIQUIDS, AN INTEGRAL APPROACH

M. M. FARAHAT
Argonne National Laboratory, Chemical Engineering Division, Argonne, IL 60439, U.S.A.

and

T. N. NASR
University of Manitoba, Department of Physics, Winnipeg, Manitoba, Canada

(*Received* 18 *February* 1976 *and in revised form* 15 *April* 1977)

NOMENCLATURE

A, area;
B, constant, equation (7);
C_p, specific heat at constant pressure;
D, diameter;
$F(\eta)$, velocity function, $= u/u_0$;
$G(\eta)$, temperature function $= (T-T_s)/(T_w-T_s)$;
Gr, Grashof number;
$I(\theta)$, integral, equation (8)
$$= \left[\int_0^\theta (\sin\theta)^{5/3}\,d\theta/(\sin\theta)^{8/3}\right]^{1/4};$$
g, acceleration of gravity;
K, thermal conductivity;
$\dot{m}$, mass flow rate, $= \rho\bar{u}\cdot 2\pi R\delta\sin\theta$;
Nu, Nusselt number;
$\overline{Nu}$, average Nusselt number, $= \frac{1}{\pi}\int_0^\pi Nu(\theta)\,d\theta$;
Pr, Prandtl number;
Pr^*, modified Prandtl number $= Pr(1+2\lambda/C_p\Delta T) = Pr(2\lambda^*/C_p\Delta T)$;
q'', heat flux;
T, temperature;
ΔT, wall superheat, $T_w - T_s$;
u, tangential component of velocity;
$\bar{u}$, average velocity, $= \frac{1}{\delta}\int_0^\delta u\,dy$;
v, radial component of velocity;
x, tangential coordinate;
y, radial coordinate.

Greek symbols

γ_1, numerical constant, $= F'(1)$;
γ_2, numerical constant, $= F'(0)$;
γ_3, numerical constant, $= G'(0)$;
γ_4, numerical constant, $= \int_0^1 F(\eta)\,d\eta$;
δ, vapor film thickness;
θ, angular coordinate;
η, dimensionless radial coordinate, $= y/\delta$;
λ, latent heat of vaporization;
λ^*, modified latent heat of vaporization, $= \lambda(1+C_p\Delta T/2\lambda)$;
ν, kinematic viscosity;
ρ, density.

Subscripts

l, liquid;
s, saturation;
w, wall.

Superscripts

$'$, differential with respect to η;
$\bar{\ }$, average value.